
Variational Auto-Regressive Gaussian Processes for Continual Learning

Sanyam Kapoor
Uber AI
sanyam@uber.com

Theofanis Karaletsos
Uber AI
theofanis@uber.com

Thang D. Bui
Uber AI
thang.bui@uber.com

Abstract

This paper proposes *Variational Auto-Regressive Gaussian Process* (VAR-GP), a principled *Bayesian* updating mechanism to incorporate new data for sequential tasks in the context of continual learning. It relies on a novel auto-regressive characterization of the variational distribution and inference is made scalable using sparse inducing point approximations. Experiments on standard continual learning benchmarks demonstrate the ability of VAR-GPs to perform well at new tasks without compromising performance on old ones, yielding competitive results to state-of-the-art methods. In addition, we qualitatively show how VAR-GP improves the predictive entropy estimates as we train on new tasks. Further, we conduct a thorough ablation study to verify the effectiveness of inferential choices.

1 Introduction

Continual Learning is the constant development of complex behaviors by building upon previously acquired skills [27, 35]. This is evident in humans and many other animals exhibit knowledge acquisition during their lifetime for skill development [12]. In the context of machine learning, much of modern success in (un)supervised learning has relied on data being *i.i.d.* However, many practical applications demand a departure from this assumption. For instance, (i) a hospital may lose access to old patient data forever for legal reasons, (ii) training on all data may be too slow for a real-time system to be updated fast enough and, (iii) privacy-conscious systems may prefer data to stay on devices instead of being sent to a third-party. We desire to keep improving our models by building on top of the previously acquired knowledge in such settings.

These settings are made challenging by data distribution shifts and conventional training methods are prone to over-fitting to the data at hand. This phenomenon has been investigated in the context of neural networks as *catastrophic forgetting* [18, 25]. The recursive application of *Bayes'* theorem provides us with a principled approach to update beliefs as new data arrives [30, 2] and much literature has been devoted to scalable *Bayesian* updating schemes – regularization using a Laplace approximation and diagonal Fisher information matrix [15] or approximate path integral of gradient vector fields [42], using recursive variational approximations [21, 34, 1], targeting adaptive capacity in *Bayesian* neural networks [14], and episodic memory-based approaches [17, 26]. Gaussian Processes (GP) have also been proposed in similar settings for online regression [7, 6], regression using streaming data [3], and functional regularization of neural networks [37]. We focus on developing an inference framework to tackle this challenge of *catastrophic forgetting*.

We propose *Variational Auto-Regressive Gaussian Processes* (VAR-GPs) for continual learning. This is facilitated by advances in variational inference and scalable sparse approximations for Gaussian Processes [36, 9, 10]. The key contributions of this work are: (1) the construction of a generalized variational lower bound for sequential datasets in a continual learning setting, (2) a novel characterization of the auto-regressive variational distributions inspired by a structured Expectation Propagation approximation and an orthogonal sparse inducing point approximation, (3) evidence on

the superior performance of using hyper-priors for sustained performance during continual learning. The paper is organized as follows - §2 puts prior work in context and §3 summarizes the necessary background. §4 develops our main proposal, VAR-GPs and §5 validates the effectiveness of VAR-GPs, including thorough ablation studies. We finally conclude with future directions in §6.

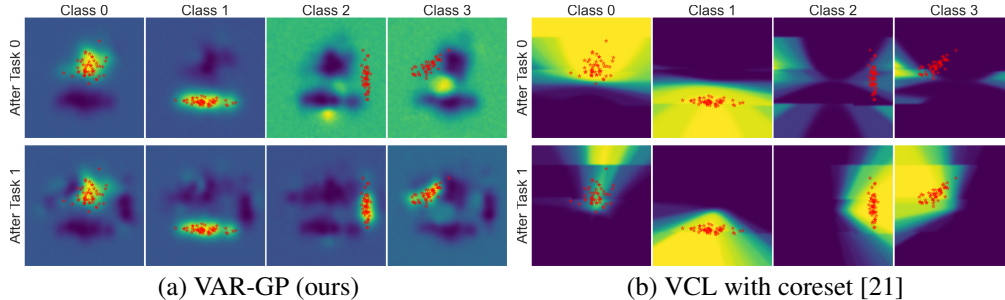


Figure 1: This figure shows class-wise output probabilities in each column for classifiers trained using a synthetic dataset (Fig. 2) on the 2-D plane $x, y \in [-3., 3.]$. The first row represents the predictive density surface after training for Task 0 (observing classes 0/1) and the second after training for Task 1 (observing classes 2/3). Brighter regions represent higher probabilities. Training points for each class are marked (*). (a) VAR-GPs show clean progression in the density space. The new data distribution is learned without disturbing much of the structure induced by the previous task. The values were computed using a Monte Carlo estimate of 50 function samples and 20 variational samples. (b) VCL (with 10 coreset points) tends to be overconfident in its predictions and is structurally less stable as the density space is disturbed, leading to worse subsequent performance.

2 Related Work

The challenge of Continual Learning (CL) is broad. Farquhar and Gal [8] and van de Ven and Tolias [38] discuss key desiderata, setup and structured evaluations for a CL system. Our work aligns with those proposals. Particularly, task identity is unknown making the problem harder (e.g. otherwise revealed via a multi-head approach). The literature focuses on one or more aspects of CL - vanilla transfer learning [16], adaptive model capacity, episodic memory and inference schemes. Reiterating, our work focuses solely on developing an inference scheme for CL.

An important body of work relies on regularization of the parameters using the previous posterior (or the prior in absence of learning) - *Elastic Weight Consolidation* (EWC) proposes Laplace and Fisher Matrix approximations [15], Ritter et al. [28] use Kronecker-factored approximated Laplace approximation, *Synaptic Intelligence* (SI) uses approximate path integral of gradient vector fields [42] and Chaudhry et al. [5] propose a Riemannian walk for CL. Variational Continual Learning (VCL) [21, 34] makes the recursive approximate posterior explicit. In contrast with our work, all these methods rely only on parameters from task $t - 1$ for regularization in task t . Other approaches indirectly related to our work also cover important aspects of CL. *Progressive Neural Networks* adapt model capacity over the course of learning by rewiring neural networks [29, 31]. Indian Buffet Process priors were introduced to adapt capacity in *Bayesian* neural networks [14]. Episodic memory has also been used to limit catastrophic forgetting in CL [33, 26] by carefully saving important data points for future tasks, as also done in VCL.

GPs have also been used for CL and are our key tool. Historically, Csató and Opper [7] and Csató [6] presented seminal works in the context of online regression. More recently, Bui et al. [3] developed a general scheme for streaming data which also relates to the general streaming variational *Bayes* framework [2]. Moreno-Muñoz et al. [19] adapt the one step recurrent approximate posterior (as in e.g. VCL) to multi-output GPs. Titsias et al. [37] leverage GPs to regularize neural networks in the functional space for CL and propose an alternate objective for inducing point selection. Our proposed inference method is complementary to these and can potentially be combined for enhanced performance.

3 Background

3.1 Gaussian Processes

Gaussian Processes (GPs) provide a flexible non-parametric framework to perform probabilistic inference [24]. The GP models a distribution over function values such that *any* finite number are Gaussian distributed. Among many desirable properties, GPs allow for tractable posterior inference (closed-form for Gaussian likelihoods) and calibrated uncertainty estimates.

In a typical regression setup, we have a dataset $\mathcal{D} = \{\mathbf{x}_i, y_i\}_{i=1}^N$ of N input and scalar-valued outputs which is assumed to be generated by an unknown mapping f with Gaussian observation noise ($\epsilon \sim \mathcal{N}(0, \sigma_y^2)$). The object of inference is f . We apply *Bayesian* reasoning by modeling the joint probability of the system ($\mathbf{y} = \{y_i\}_{i=1}^N; \mathbf{X} = \{\mathbf{x}_i\}_{i=1}^N; f$) as

$$f|\mathbf{X}, \boldsymbol{\theta} \sim \mathcal{GP}(m(\mathbf{X}), \kappa^\theta(\mathbf{X})) = \mathcal{N}(m(\mathbf{X}), \mathbf{K}^\theta(\mathbf{X}, \mathbf{X})), \quad (1)$$

$$p(\mathbf{y}, f|\mathbf{X}, \boldsymbol{\theta}) = p(f|\mathbf{X}, \boldsymbol{\theta}) \prod_{i=1}^N p(y_i|f, \mathbf{x}_i) \quad (2)$$

\mathcal{GP} represents the prior over functions. $m(\mathbf{X})$ is the mean function and is considered to be $\mathbf{0}$ in this work though other choices are possible. $\kappa_\theta \in \mathbb{R}^{N \times N}$ is a positive definite kernel, depending on hyperparameters $\boldsymbol{\theta}$, which induces a covariance matrix such that $\mathbf{K}_{i,j}^\theta = \kappa^\theta(\mathbf{x}_i, \mathbf{x}_j)$. $p(y|f, \mathbf{x})$ is the likelihood function – in this regression problem, we assume a Gaussian likelihood (observation noise). Consequently, for test data \mathbf{X}_* , the exact posterior $p(f_*|\mathbf{X}_*, \mathbf{X}, \mathbf{y}) = \mathcal{N}(f_*; \boldsymbol{\mu}_*, \boldsymbol{\Sigma}_*)$ ¹ can now be recovered as follows,

$$\begin{aligned} \boldsymbol{\mu}_* &= \mathbf{K}^\theta(\mathbf{X}_*, \mathbf{X})^\top (\mathbf{K}^\theta(\mathbf{X}, \mathbf{X}) + \sigma_y^2 \mathbf{I})^{-1} \mathbf{y}, \\ \boldsymbol{\Sigma}_* &= \mathbf{K}^\theta(\mathbf{X}_*, \mathbf{X}_*) - \mathbf{K}^\theta(\mathbf{X}_*, \mathbf{X})^\top (\mathbf{K}^\theta(\mathbf{X}, \mathbf{X}) + \sigma_y^2 \mathbf{I})^{-1} \mathbf{K}^\theta(\mathbf{X}, \mathbf{X}_*). \end{aligned} \quad (3)$$

The kernel hyperparameters and observation noise can be learnt by finding a local maximum of the marginal likelihood $p(\mathbf{y}|\mathbf{X}, \boldsymbol{\theta}, \sigma_y^2) = \int p(\mathbf{y}|\mathbf{X}, f, \sigma_y^2) p(f|\mathbf{X}, \boldsymbol{\theta}) df = \mathcal{N}(\mathbf{y}; \mathbf{0}, \mathbf{K}^\theta(\mathbf{X}, \mathbf{X}) + \sigma_y^2 \mathbf{I})$.

For a K -way classification problem, K independent GP functions are passed through a *softmax* function. It should be noted that inference does not remain closed-form and must be approximated (e.g. via Monte Carlo). Similarly, an introduction of hyper-priors over $\boldsymbol{\theta}$ also does not allow closed-form posterior and thus requires either asymptotically exact sampling or approximate inference. Even when the exact posterior is available as in GP regression with a Gaussian likelihood, scaling to large datasets is computationally expensive, because of the $\mathcal{O}(N^3)$ complexity of the marginal likelihood computation and $\mathcal{O}(N^2)$ complexity for each test output computation. Sparse approximations are thus often resorted to, to sidestep the aforementioned analytical and computational intractabilities.

3.2 Sparse Variational Gaussian Processes

There are a plethora of sparse approximations for efficient inference and learning in Gaussian Process model. This section focuses on pseudo-point based methods [23, 4] and, in particular, the seminal work of Titsias [36], Hensman et al. [9, 10] as this forms the basis of the proposed continual learning algorithm. We consider a subset of M function values $\mathbf{u} = \{u_i\}_{i=1}^M$ from the infinite-dimensional object $f = \{f_{\neq \mathbf{u}}, \mathbf{u}\}$ induced by a new set of inputs called pseudo-inputs or inducing points $\mathbf{Z} = \{\mathbf{z}_i\}_{i=1}^M$. We can now rewrite the system joint in (2) as

$$p(\mathbf{y}, f|\mathbf{X}, \boldsymbol{\theta}) = p(\mathbf{u}|\mathbf{Z}, \boldsymbol{\theta}) p(f_{\neq \mathbf{u}}|\mathbf{X}, \mathbf{u}, \mathbf{Z}, \boldsymbol{\theta}) p(\mathbf{y}|f, \mathbf{X}) \quad (4)$$

For approximate inference of the posterior over f , we posit the variational distribution to be factored as $q(f) = q(\mathbf{u})p(f_{\neq \mathbf{u}}|\mathbf{X}, \mathbf{u}, \mathbf{Z}, \boldsymbol{\theta})$.² This leads to a tractable expression for the variational lower bound to the log marginal likelihood [13] owing to cancellation of key terms as follows,

¹Going forward, we will replace $\mathbf{K}^\theta(\mathbf{X}, \mathbf{Y}) \leftrightarrow \mathbf{K}_{\mathbf{X}, \mathbf{Y}}$, making the dependence on $\boldsymbol{\theta}$ implicit.

²In what follows, the dependence on \mathbf{X} and \mathbf{Z} will be made implicit when appropriate, e.g. $p(f_{\neq \mathbf{u}}|\mathbf{X}, \mathbf{u}, \mathbf{Z}, \boldsymbol{\theta}) \leftrightarrow p(f_{\neq \mathbf{u}}|\mathbf{u}, \boldsymbol{\theta})$ and $p(\mathbf{u}|\mathbf{Z}, \boldsymbol{\theta}) \leftrightarrow p(\mathbf{u}|\boldsymbol{\theta})$.

$$\mathcal{F}(q) = \mathbb{E}_{q(f)} \left[\log \frac{p(\mathbf{u}|\boldsymbol{\theta}) p(f_{\neq \mathbf{u}}|\mathbf{u}, \boldsymbol{\theta}) p(\mathbf{y}|f, \mathbf{X})}{q(\mathbf{u}) p(f_{\neq \mathbf{u}}|\mathbf{u}, \boldsymbol{\theta})} \right] = \sum_{i=1}^N \mathbb{E}_{q(f)} [\log p(y_i|f, \mathbf{x}_i)] - \mathcal{KL}[q(\mathbf{u})||p(\mathbf{u}|\boldsymbol{\theta})].$$

In addition, this allows for stochastic variational inference [11, 9] - noisy but unbiased estimates via dataset sub-sampling for the likelihood term (with appropriate scaling). Bui et al. [3] employed this variational formulation to handle streaming data, extending earlier work [7]. However, these approaches have undesirable performance on modern continual learning benchmarks – the inducing points are either too rigid to adapt to new data or move too quickly leading to catastrophic forgetting.

4 Variational Auto-Regressive Gaussian Processes

We now introduce the main proposal, *Variational Auto-Regressive Gaussian Processes*, in the context of continual learning. Consider a general setting in which datasets $\{\mathcal{D}^{(t)}\}_{t=1}^T$ arrive sequentially for T different but related tasks such that we see the dataset only once (e.g. due to memory or computational constraints). We desire to build a model which can incorporate data online and perform well on the incoming task without considerably compromising performance on old tasks. The dataset of size N_t at time $t \in [1, T]$ is represented as $\mathcal{D}^{(t)} = \{\mathbf{x}_i^{(t)}, y_i^{(t)}\}_{i=1}^{N_t}$.

4.1 Learning the first task

Learning the first task using $\mathcal{D}^{(1)}$ can be done in the usual manner with Sparse Variational GPs (see §3). Although, an important modeling choice where we differ from standard approaches and imperative to the success of the method is to be *Bayesian* about the hyperparameters. Extending the system joint in (4) along with appropriate task identifiers gives the following joint density,

$$p(\mathbf{y}^{(1)}, f, \boldsymbol{\theta} | \mathbf{X}^{(1)}) = p(\boldsymbol{\theta}) p(\mathbf{u}_1 | \mathbf{Z}_1, \boldsymbol{\theta}) p(f_{\neq \mathbf{u}_1} | \mathbf{X}^{(1)}, \mathbf{u}_1, \mathbf{Z}_1, \boldsymbol{\theta}) \prod_{i=1}^{N_1} p(y_i^{(1)} | f, \mathbf{x}_i^{(1)}). \quad (5)$$

We posit a variational distribution $q_1(f, \boldsymbol{\theta}) = q_1(\boldsymbol{\theta}) q(\mathbf{u}_1) p(f_{\neq \mathbf{u}_1} | \mathbf{X}^{(1)}, \mathbf{u}_1, \mathbf{Z}_1, \boldsymbol{\theta})$, leading to the following variational lower bound

$$\mathcal{F}(q_1) = \sum_{i=1}^{N_1} \mathbb{E}_{q_1(f, \boldsymbol{\theta})} [\log p(y_i^{(1)} | f, \mathbf{x}_i^{(1)})] - \mathcal{KL}[q_1(\boldsymbol{\theta}) || p(\boldsymbol{\theta})] - \mathbb{E}_{q_1(\boldsymbol{\theta})} [\mathcal{KL}[q(\mathbf{u}_1) || p(\mathbf{u}_1 | \boldsymbol{\theta})]]. \quad (6)$$

4.2 Generalized Continual Variational Lower Bound

For all tasks $t > 1$, we manipulate the infinite-dimensional object, $f = \{f_{\neq \mathbf{u}_{\leq t}}, \mathbf{u}_{< t}, \mathbf{u}_t\}$. $\mathbf{u}_{< t}$ represents the set of function values at all past inducing points, $\{\mathbf{u}_j\}_{j=1}^{t-1}$. The approximate system joint for subsequent tasks can be now written using the approximate posteriors recovered from old tasks conditioned on previously seen datasets $\mathcal{D}^{(<t)} = \{\mathcal{D}^{(j)}\}_{j=1}^{t-1}$ as

$$p(\mathbf{y}^{(t)}, f, \boldsymbol{\theta} | \mathbf{X}^{(t)}, \mathcal{D}^{(<t)}) \approx q_{t-1}(\boldsymbol{\theta}) q(\mathbf{u}_{< t} | \mathbf{Z}_{< t}, \boldsymbol{\theta}) p(\mathbf{u}_t | \mathbf{Z}_t, \mathbf{u}_{< t}, \mathbf{Z}_{< t}, \boldsymbol{\theta}) p(f_{\neq \mathbf{u}_{\leq t}} | \mathbf{X}^{(t)}, \mathbf{u}_{\leq t}, \mathbf{Z}_{\leq t}, \boldsymbol{\theta}) \prod_{i=1}^{N_t} p(y_i^{(t)} | f, \mathbf{x}_i^{(t)}). \quad (7)$$

We posit a structured variational distribution to mirror the joint density, consequently leading to the generalized continual variational lower bound ³,

³Going forward, we will make dependence on \mathbf{Z} implicit. e.g. $q(\mathbf{u}_{< t} | \mathbf{Z}_{< t}, \boldsymbol{\theta}) \leftrightarrow q(\mathbf{u}_{< t} | \boldsymbol{\theta})$, $q(\mathbf{u}_t | \mathbf{Z}_t, \mathbf{u}_{< t}, \mathbf{Z}_{< t}, \boldsymbol{\theta}) \leftrightarrow q(\mathbf{u}_t | \mathbf{u}_{< t}, \boldsymbol{\theta})$, and so on.

$$q_t(f, \boldsymbol{\theta}) = q_t(\boldsymbol{\theta})q(\mathbf{u}_{<t}|\mathbf{Z}_{<t}, \boldsymbol{\theta})q(\mathbf{u}_t|\mathbf{Z}_t, \mathbf{u}_{<t}, \mathbf{Z}_{<t}, \boldsymbol{\theta})p(f_{\neq \mathbf{u}_{\leq t}}|\mathbf{X}^{(t)}, \mathbf{u}_{\leq t}, \mathbf{Z}_{\leq t}, \boldsymbol{\theta}), \quad (8)$$

$$\begin{aligned} \mathcal{F}(q_t) &= \sum_{i=1}^{N_t} \mathbb{E}_{q_t(f, \boldsymbol{\theta})} \left[\log p\left(y_i^{(t)}|f, \mathbf{x}_i^{(t)}\right) \right] - \mathcal{KL} [q_t(\boldsymbol{\theta})||q_{t-1}(\boldsymbol{\theta})] \\ &\quad - \mathbb{E}_{q_t(\boldsymbol{\theta})q(\mathbf{u}_{<t}|\mathbf{Z}_{<t}, \boldsymbol{\theta})} \left[\mathcal{KL} [q(\mathbf{u}_t|\mathbf{Z}_t, \mathbf{u}_{<t}, \mathbf{Z}_{<t}, \boldsymbol{\theta})||p(\mathbf{u}_t|\mathbf{Z}_t, \mathbf{u}_{<t}, \mathbf{Z}_{<t}, \boldsymbol{\theta})] \right]. \quad (9) \end{aligned}$$

The maximization of this bound takes a natural interpretation - the first term maximizes the likelihood of the current dataset $\mathcal{D}^{(t)}$ while being regularized by the conditional prior over inducing points to preserve information gained by the previous inducing points, as $\mathbf{Z}_{<t}$ remain fixed. The regularization over the hyperparameters provides a further signal to avoid over-fitting to the current task.

4.3 Distributional choices

We now present the precise parametrizations for all the distributions. In particular, our proposed parametrization of $q(\mathbf{u}_t|\mathbf{u}_{<t}, \boldsymbol{\theta})$ is essential for sustained performance over many tasks and the precise form is justified towards the end.

For the prior model, $p(\mathbf{u}_1|\boldsymbol{\theta})$, $p(\mathbf{u}_t|\mathbf{u}_{<t}, \boldsymbol{\theta})$ and $p(f_{\mathbf{u}_{\leq t}}|\mathbf{X}^{(t)}, \mathbf{u}_{\leq t}, \boldsymbol{\theta})$ can be computed by invoking the GP prior. All experiments use the Exponentiated Quadratic kernel such that $\boldsymbol{\theta}$ includes the ARD lengthscales and a scale factor. The prior over the hyperparameters for the first task $p(\boldsymbol{\theta})$ is assumed to be a standard Normal $\mathcal{N}(\boldsymbol{\theta}; \mathbf{0}, \mathbf{I})$ and the variational distribution of the hyperparameters is assumed to be a mean-field Gaussian $q_t(\boldsymbol{\theta}) = \mathcal{N}(\boldsymbol{\theta}; \boldsymbol{\mu}_t, \text{diag}(\boldsymbol{\sigma}_t))$. These choices allow for closed-form \mathcal{KL} computations in (6) and (9).

The variational distribution over inducing points for the first task is parametrized as $q(\mathbf{u}_1) = \mathcal{N}(\mathbf{u}_1; \mathbf{m}_1, \boldsymbol{\Sigma}_1)$, as in standard sparse variational GP implementations, where $\mathbf{m}_1 \in \mathbb{R}^{M_1}$ is the mean and $\boldsymbol{\Sigma}_1$ is the full covariance matrix $\mathbb{R}^{M_1 \times M_1}$ for a set of M_1 inducing points of the first task. For all subsequent tasks $t > 1$, we use an auto-regressive parametrization for the variational distribution given by $q(\mathbf{u}_{<t}|\boldsymbol{\theta}) = q(\mathbf{u}_1) \prod_{j=2}^{t-1} q(\mathbf{u}_j|\mathbf{u}_{<j}, \boldsymbol{\theta})$ and $q(\mathbf{u}_t|\mathbf{u}_{<t}, \boldsymbol{\theta}) = \mathcal{N}(\mathbf{u}_t; \mathbf{K}_{\mathbf{Z}_t, \mathbf{Z}_{<t}} \mathbf{K}_{\mathbf{Z}_{<t}, \mathbf{Z}_{<t}}^{-1} \mathbf{u}_{<t} + \mathbf{m}_t, \boldsymbol{\Sigma}_t)$. An interesting consequence of this choice is that the \mathcal{KL} -divergence between inducing points becomes independent of $\mathbf{u}_{<t}$ and hence avoid using many samples from $q(\mathbf{u}_{<t}|\boldsymbol{\theta})$. We provide two justifications for this choice.

4.3.1 Structured EP factor approximation leads to an auto-regressive approximate posterior

Recall the following running joint density that we wish to approximate:

$$p(\mathbf{y}^{(t)}, f, \boldsymbol{\theta}|\mathbf{X}^{(t)}, \mathcal{D}^{(<t)}) \approx q_{t-1}(\boldsymbol{\theta})q(\mathbf{u}_{<t}|\boldsymbol{\theta})p(\mathbf{u}_t|\mathbf{u}_{<t}, \boldsymbol{\theta})p(f_{\neq \mathbf{u}_{\leq t}}|\mathbf{u}_{\leq t}, \boldsymbol{\theta}) \prod_{i=1}^{N_t} p(y_i^{(t)}|f, \mathbf{x}_i^{(t)}).$$

We can introduce an approximation to the posterior as follows,

$$q_t(f, \boldsymbol{\theta}) \propto q_{t-1}(\boldsymbol{\theta})q(\mathbf{u}_{<t}|\boldsymbol{\theta})p(\mathbf{u}_t|\mathbf{u}_{<t}, \boldsymbol{\theta})p(f_{\neq \mathbf{u}_{\leq t}}|\mathbf{u}_{\leq t}, \boldsymbol{\theta}) \prod_{i=1}^{N_t} \mathbf{g}_i^{(t)}(\boldsymbol{\theta})\mathbf{h}_i^{(t)}(\mathbf{u}_i),$$

where the difficult likelihood term, $\prod_{i=1}^{N_t} p(y_i^{(t)}|f, \mathbf{x}_i^{(t)})$, is approximated by $\prod_{i=1}^{N_t} \mathbf{g}_i^{(t)}(\boldsymbol{\theta})\mathbf{h}_i^{(t)}(\mathbf{u}_i)$ - \mathbf{g} and \mathbf{h} are the approximate contributions of each likelihood term to the posterior. EP then proceeds by repeating until convergence: for the i -th datum, (i) remove the approximate contributions \mathbf{g}_i and \mathbf{h}_i from the posterior to form the cavity, (ii) merging the cavity with $p(y_i^{(t)}|f, \mathbf{x}_i^{(t)})$ to form the tilted distribution \tilde{p}_i , (iii) minimize the divergence $\text{KL}[\tilde{p}_i||q_t]$ to find a new approximate posterior, and (iv) obtain the new approximate factors \mathbf{g}_i and \mathbf{h}_i by removing the cavity from the new posterior.

However, we are not interested in running EP, but only in the form of the approximate posterior induced by the EP factor approximation above. In particular, we can merge the relevant terms in the approximate posterior as follows,

$$q_t(f, \boldsymbol{\theta}) \propto q_t(\boldsymbol{\theta})q(\mathbf{u}_{<t}|\boldsymbol{\theta})q(\mathbf{u}_t|\mathbf{u}_{<t}, \boldsymbol{\theta})p(f_{\neq \mathbf{u}_{<t}}|\mathbf{u}_{<t}, \boldsymbol{\theta})$$

where $q_t(\boldsymbol{\theta}) \propto q_{t-1}(\boldsymbol{\theta}) \prod_{i=1}^{N_t} \mathbf{g}_i^{(t)}(\boldsymbol{\theta})$ and $q(\mathbf{u}_t|\mathbf{u}_{<t}, \boldsymbol{\theta}) \propto p(\mathbf{u}_t|\mathbf{u}_{<t}, \boldsymbol{\theta}) \prod_{i=1}^{N_t} \mathbf{h}_i^{(t)}(\mathbf{u}_t)$. We note that, $p(\mathbf{u}_t|\mathbf{u}_{<t}, \boldsymbol{\theta}) = \mathcal{N}(\mathbf{u}_t; \mathbf{A}_t \mathbf{u}_{<t}, \mathbf{C}_t)$, where $\mathbf{A}_t = \mathbf{K}_{\mathbf{z}_t, \mathbf{z}_{<t}} \mathbf{K}_{\mathbf{z}_{<t}, \mathbf{z}_{<t}}^{-1}$, and $\mathbf{C}_t = \mathbf{K}_{\mathbf{z}_t, \mathbf{z}_t} - \mathbf{K}_{\mathbf{z}_t, \mathbf{z}_{<t}} \mathbf{K}_{\mathbf{z}_{<t}, \mathbf{z}_{<t}}^{-1} \mathbf{K}_{\mathbf{z}_{<t}, \mathbf{z}_t}$. We consider a Gaussian factor approximation, $\mathbf{H}_t(\mathbf{u}_t) = \prod_{i=1}^{N_t} \mathbf{h}_i^{(t)}(\mathbf{u}_t) = \mathcal{N}(\mathbf{u}_t; \boldsymbol{\mu}, \boldsymbol{\Sigma})$. Multiplying $\mathbf{H}_t(\mathbf{u}_t)$ with $p(\mathbf{u}_t|\mathbf{u}_{<t}, \boldsymbol{\theta})$ and renormalizing give $q(\mathbf{u}_t|\mathbf{u}_{<t}, \boldsymbol{\theta}) = \mathcal{N}(\mathbf{u}_t; \tilde{\boldsymbol{\mu}}, \tilde{\boldsymbol{\Sigma}})$, where $\tilde{\boldsymbol{\Sigma}}^{-1} = \boldsymbol{\Sigma}^{-1} + \mathbf{C}_t^{-1}$ and $\tilde{\boldsymbol{\Sigma}}^{-1} \tilde{\boldsymbol{\mu}} = \boldsymbol{\Sigma}^{-1} \boldsymbol{\mu} + \mathbf{C}_t^{-1} \mathbf{A}_t \mathbf{u}_{<t}$. We can further rewrite the conditional posterior mean as $\tilde{\boldsymbol{\mu}} = \mathbf{A}_t \mathbf{u}_{<t} + (\mathbf{I} + \boldsymbol{\Sigma} \mathbf{C}_t^{-1})^{-1} (\boldsymbol{\mu} - \mathbf{A}_t \mathbf{u}_{<t})$. This means that instead of parametrizing the factor $\mathbf{H}_t(\mathbf{u}_t)$, we can use an equivalent parametrization of the conditional posterior, $q(\mathbf{u}_t|\mathbf{u}_{<t}, \boldsymbol{\theta}) = \mathcal{N}(\mathbf{u}_t; \mathbf{A}_t \mathbf{u}_{<t} + \mathbf{m}, \boldsymbol{\Sigma})$.

4.3.2 Equivalence to orthogonal inducing points

We note that the proposed auto-regressive parametrization is exactly equivalent to the orthogonal inducing point formulation when $T = 2$ [32, §3.3]. A variational approximation over two set of *orthogonal* inducing points, \mathbf{u} and \mathbf{v} is presented as

$$q(\mathbf{u}, \mathbf{v}) = \mathcal{N} \left(\begin{bmatrix} \mathbf{u} \\ \mathbf{v} \end{bmatrix}; \begin{bmatrix} \mathbf{m}_u \\ \mathbf{K}_{\mathbf{v}\mathbf{u}} \mathbf{K}_{\mathbf{u}\mathbf{u}}^{-1} \mathbf{m}_u \end{bmatrix}, \begin{bmatrix} \boldsymbol{\Sigma}_u & \boldsymbol{\Sigma}_u \mathbf{K}_{\mathbf{u}\mathbf{u}}^{-1} \mathbf{K}_{\mathbf{u}\mathbf{v}} \\ \mathbf{K}_{\mathbf{v}\mathbf{u}} \mathbf{K}_{\mathbf{v}\mathbf{v}}^{-1} \boldsymbol{\Sigma}_u & \boldsymbol{\Sigma}_v + \mathbf{K}_{\mathbf{v}\mathbf{u}} \mathbf{K}_{\mathbf{u}\mathbf{u}}^{-1} \boldsymbol{\Sigma}_u \mathbf{K}_{\mathbf{u}\mathbf{v}}^{-1} \mathbf{K}_{\mathbf{u}\mathbf{v}} \end{bmatrix} \right).$$

We note that this can be rewritten as,

$$q(\mathbf{u}, \mathbf{v}) = q(\mathbf{u})q(\mathbf{v}|\mathbf{u}) = \mathcal{N}(\mathbf{u}; \mathbf{m}_u, \boldsymbol{\Sigma}_u) \mathcal{N}(\mathbf{v}; \mathbf{K}_{\mathbf{v}\mathbf{u}} \mathbf{K}_{\mathbf{u}\mathbf{u}}^{-1} \mathbf{u} + \mathbf{m}_v, \boldsymbol{\Sigma}_v),$$

which is equivalent to the proposed autoregressive parametrization when there are two time steps, and $\mathbf{u} \Leftrightarrow \mathbf{u}_1$ and $\mathbf{v} \Leftrightarrow \mathbf{u}_2$. Intuitively speaking, the second set of inducing points attempts to cover or explain the data that is not well-explained by the first set. The key difference between the two works is that the proposed approximation in this paper is applied to the continual learning setting and uses many sets of inducing points corresponding to many continual learning steps, instead of two sets and the batch setting of Shi et al. [32].

5 Experiments

We evaluate the performance of VAR-GPs and compare it with a state-of-the-art approach - Variational Continual Learning (VCL) [21, 34]. The proposed method has been implemented in PyTorch [22]⁴. We also conduct a thorough ablation study and verify the effectiveness of proposed modeling choices.

In all experiments, the model only observes $\mathcal{D}^{(t)}$ for training but is tested on all the tasks seen so far using $\mathcal{D}^{(\leq t)}$. A subset of the training set is used as a validation set for early stopping using the validation accuracy, with a maximum of 500 training epochs. Yogi [41] is used as the optimizer with a mini-batch size of 512 for the computation of (6) and (9). We use a tempered version of the lower bound and penalize the \mathcal{KL} -divergence of hyperparameters using a scalar β as has been commonly noted in literature [39] for better performance. All numbers are reported based on one standard deviation after five independent trials. We describe the datasets used for experiments below.

Synthetic Classification Dataset A synthetic 4-way classification dataset which occupies the 2-D space $x, y \in [-3., 3.]$ as in Fig. 2, allows us to visualize the qualitative characteristics of VAR-GPs.

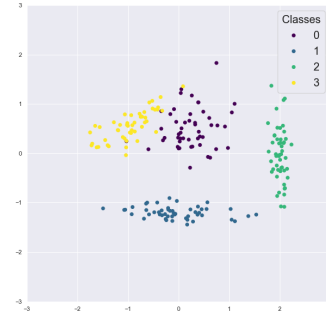


Figure 2: Synthetic Dataset

⁴Complete code is available at bit.ly/var-gp-code.

Table 1: This table provides the final average test accuracy (in %) after training on all tasks – 5 for Split MNIST and 10 for Permuted MNIST in a continual learning setting (see §5). The results are averaged over five independent trials and we include one standard error (where available). *Split MNIST results for SI [42] and EWC [15] are taken from VCL [34] however are not directly comparable as they use a multi-head setup making evaluation easier; CS = coreset.

Method	Split MNIST	Permuted MNIST
SI	98.9*	86.02
EWC	63.1*	84.11
VCL, [100]	19.90 ± 0.14	82.94 ± 0.85
+ CS(50)	76.21 ± 2.02	85.80 ± 0.41
+ CS(100)	81.90 ± 1.64	86.45 ± 0.26
VCL, [100, 100]	19.91 ± 7.79	94.31 ± 1.05
+ CS(50)	71.89 ± 5.06	95.43 ± 0.39
+ CS(100)	75.54 ± 1.06	95.06 ± 0.22
VAR-GP (ours)	90.57 ± 1.06	97.20 ± 0.08
+ Block Diagonal	78.64 ± 1.41	96.31 ± 0.42
+ MLE Hypers	10.09 ± 0.40	10.07 ± 0.15
+ Global	39.31 ± 0.28	46.02 ± 1.09

Split MNIST This benchmark was used to evaluate Synaptic Intelligence [42]. At each timestep, we consider the full 10-way classification task but receive a dataset $\mathcal{D}^{(t)}$ of only a subset of MNIST digits in the sequence 0/1, 2/3, 4/5, 6/7 and 8/9. A key distinction from prior work is that we do not use a multi-head setup to report the classification test accuracy which aligns with the desiderata outlined by Farquhar and Gal [8]. 10000 training samples are set aside for validation cumulatively across all tasks. We use $M_t = M = 60$ inducing points, a learning rate of 0.003 and, $\beta = 10.0$.

Permuted MNIST In this benchmark, we receive a dataset $\mathcal{D}^{(t)}$ of MNIST digits at each timestep t where the pixels undergo a fixed permutation. While neural network-based approaches [42, 15] utilize this benchmark as an indicator of representational capacity, the benchmark remains relevant to check performance under distributional shift. The first task has been kept as the unpermuted MNIST to provide an upper bound on the asymptotic performance of subsequent tasks. 10000 samples are used for validation. We use $M_t = M = 100$ inducing points, a learning rate of 0.0037 and, $\beta = 1.64$.

5.1 Continual Learning Performance

We first visualize the synthetic dataset (Fig. 2) and see how VAR-GP carves up the decision space compared to VCL, as we start seeing data from different parts of the input space (Fig. 1). The test performance of VAR-GP and VCL as we keep adding new tasks for both Split MNIST and Permuted MNIST is compared in Fig. 3. VAR-GP is able to maintain consistent performance new tasks without compromising much performance on the old tasks. Quantitative comparisons are provided in Table 1.

Visualizing Inducing Points During training, the inducing points are initialized at a random subset of the training dataset. As the inducing points live in the input space, we can visualize a random subset after each task. We do this for Split MNIST in Fig. 4. The inducing points show a clear emergent structure and are representative of the digits associated with the current task.

Predictive Entropies Predictive entropy is a reasonable measure of uncertainty. Fig. 5 allows for a qualitative comparison of “forgetting” in VAR-GPs and VCL.

5.2 Ablations

Block Diagonal Variational Distribution Instead of the auto-regressive posterior $q(\mathbf{u}_t | \mathbf{u}_{<t}, \boldsymbol{\theta}) = \mathcal{N}(\mathbf{u}_t; \mathbf{K}_{\mathbf{z}_t, \mathbf{z}_{<t}} \mathbf{K}_{\mathbf{z}_{<t}, \mathbf{z}_{<t}}^{-1} \mathbf{u}_{<t} + \mathbf{m}_t, \boldsymbol{\Sigma}_t)$, we choose a simpler variational distribution given by $q'(\mathbf{u}_t | \mathbf{u}_{<t}, \boldsymbol{\theta}) = \mathcal{N}(\mathbf{u}_t; \mathbf{m}_t, \boldsymbol{\Sigma}_t)$ keeping all other choices the same. Effectively, removing the conditioning induces a block diagonal structure in the covariance matrix among the inducing points where each block represents the covariance among the inducing points for a given task. This also

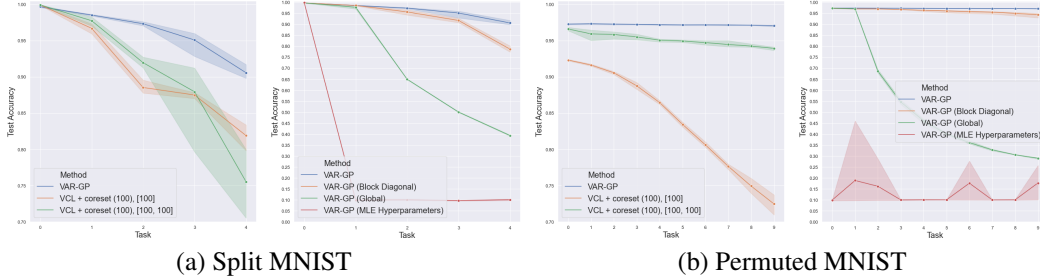


Figure 3: These graphs compare the average test accuracy of VAR-GPs to variants of VCL [21]. We also compare to alternatives within VAR-GP to validate the effectiveness of modeling choices. VAR-GPs maintain consistent performance on newer tasks without losing further performance on old tasks. For a complete list of comparisons, see Table 1.

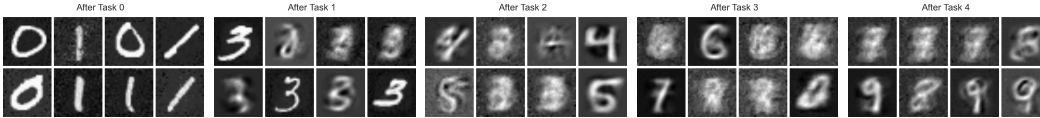


Figure 4: Visualizing inducing points in Split MNIST. The inducing points are representative of the current task.

decouples the inducing points and the hyperparameters in the approximate posterior. We hypothesize that this is detrimental to performance and is validated by Fig. 3.

Global Inducing Points An alternative characterization of the distribution is where we completely do away with the auto-regressive nature of the variational distribution and just rely on a single set of inducing points at each time step $q_t(f, \theta) = q_t(\theta)p(f_{\neq \mathbf{u}_t} | \mathbf{u}_t, \theta)q(\mathbf{u}_t)$. This variational distribution for the inducing points and an MLE estimate of the hyperparameters were previously used for streaming regression tasks [3]. However, the experimental evidence in Fig. 3 shows that such variational approximation is poor for large scale continual classification tasks. See Appendix B.1 for precise modeling details.

MLE Hyperparameters Being *Bayesian* about the hyperparameters considerably helps the model to perform well across tasks without a detrimental effect on the old ones. In this section, we validate this hypothesis by simply switching off the \mathcal{KL} -divergence term for the hyperparameters in both (6) and (9). Instead, we simply rely on a point estimate of the hyperparameters and use the maximum likelihood estimate at each step. The stark performance comparison is shown in Fig. 3. The hyper-parameters are stuck in a local minimum and virtually never recover during subsequent tasks.

Retraining old inducing points We also investigate a variant of VAR-GP named Re-VAR-GP where unlike earlier, we retrain the old inducing points $\mathbf{Z}_{<t}$. This changes the form of the variational lower bound. The precise details and implications are discussed in Appendix B.2, owing to which we do not pursue this approach further.

6 Summary and Future Directions

This work presents VAR-GPs, a *Bayesian* inference scheme for continual learning which can sustain performance over multiple tasks without being detrimental to old ones. The efficacy of modeling choices is verified by thorough experiments and ablation studies. The use of stochastic optimization allows us to scale this to large datasets. We also justify the proposed variational parametrization by drawing parallels to EP and orthogonal inducing points. There are many exciting directions to further this work. In its current form, the model grows linearly in the number of tasks. Information distillation can allow faster execution times by facilitating sub-linear growth. The representational power of VAR-GPs can be improved by the use of deep kernel learning. However, it introduces new regularization challenges to be tackled. Contemporary approaches relying on a memory buffer

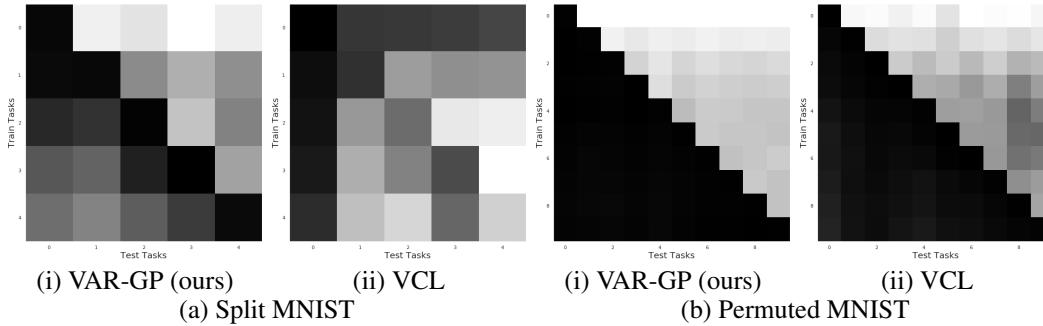


Figure 5: These graphs show the evolution of predictive entropy over the course of training tasks. Each row corresponds to the task being trained on and each column represents the mean predictive entropy for every task. In other words, the upper triangular region shows tasks which aren’t yet seen during training. The values are normalized (by maximum entropy of a ten-way classifier, $\log 10$) and brighter regions correspond to higher values. VAR-GPs are able to maintain lower predictive entropy in the lower triangular regions hinting at low forgetting rates and higher entropy in upper triangular regions as compared to VCL [21].

are also amenable to the proposed inference scheme. Finally, it is also interesting to consider the implications of our method to reinforcement learning where dataset shift is apparent.

Acknowledgements

We would like to thank Matthias Poloczek for insightful conversations along the way. SK was supported by the Uber AI Residency program.

References

- [1] Hongjoon Ahn, Sungmin Cha, Donggyu Lee, and Taesup Moon. Uncertainty-based continual learning with adaptive regularization. In *Advances in Neural Information Processing Systems*, pages 4394–4404, 2019.
- [2] Tamara Broderick, Nicholas Boyd, Andre Wibisono, Ashia C Wilson, and Michael I Jordan. Streaming variational Bayes. In *Advances in Neural Information Processing Systems*, pages 1727–1735, 2013.
- [3] Thang D Bui, Cuong Nguyen, and Richard E Turner. Streaming sparse Gaussian process approximations. In *Advances in Neural Information Processing Systems*, pages 3299–3307, 2017.
- [4] Thang D Bui, Josiah Yan, and Richard E Turner. A unifying framework for Gaussian process pseudo-point approximations using power expectation propagation. *The Journal of Machine Learning Research*, 18(1):3649–3720, 2017.
- [5] Arslan Chaudhry, Puneet K Dokania, Thalaiyasingam Ajanthan, and Philip HS Torr. Riemannian walk for incremental learning: Understanding forgetting and intransigence. In *Proceedings of the European Conference on Computer Vision*, pages 532–547, 2018.
- [6] Lehel Csató. *Gaussian processes: iterative sparse approximations*. PhD thesis, Aston University, 2002.
- [7] Lehel Csató and Manfred Opper. Sparse on-line Gaussian processes. *Neural computation*, 14(3):641–668, 2002.
- [8] Sebastian Farquhar and Yarin Gal. Towards robust evaluations of continual learning. *arXiv preprint arXiv:1805.09733*, 2018.
- [9] James Hensman, Nicolò Fusi, and Neil D. Lawrence. Gaussian processes for big data. In *29th Conference on Uncertainty in Artificial Intelligence*, page 282–290, 2013.

- [10] James Hensman, Alexander G D G Matthews, and Zoubin Ghahramani. Scalable variational Gaussian process classification. In *18th International Conference on Artificial Intelligence and Statistics*, pages 1–9, 2015.
- [11] Matthew D Hoffman, David M Blei, Chong Wang, and John Paisley. Stochastic variational inference. *The Journal of Machine Learning Research*, 14(1):1303–1347, 2013.
- [12] William Hoppitt and Kevin N Laland. *Social learning: an introduction to mechanisms, methods, and models*. Princeton University Press, 2013.
- [13] Michael I Jordan, Zoubin Ghahramani, Tommi S Jaakkola, and Lawrence K Saul. An introduction to variational methods for graphical models. *Machine learning*, 37(2):183–233, 1999.
- [14] Samuel Kessler, Vu Nguyen, Stefan Zohren, and Stephen Roberts. Hierarchical Indian buffet neural networks for Bayesian continual learning. *arXiv*, pages arXiv–1912, 2019.
- [15] James Kirkpatrick, Razvan Pascanu, Neil Rabinowitz, Joel Veness, Guillaume Desjardins, Andrei A Rusu, Kieran Milan, John Quan, Tiago Ramalho, Agnieszka Grabska-Barwinska, et al. Overcoming catastrophic forgetting in neural networks. *Proceedings of the National Academy of Sciences*, 114(13):3521–3526, 2017.
- [16] Zhizhong Li and Derek Hoiem. Learning without forgetting. *IEEE transactions on Pattern Analysis and Machine Intelligence*, 40(12):2935–2947, 2017.
- [17] David Lopez-Paz and Marc’ Aurelio Ranzato. Gradient episodic memory for continual learning. In *Advances in Neural Information Processing Systems*, pages 6467–6476, 2017.
- [18] Michael McCloskey and Neal J Cohen. Catastrophic interference in connectionist networks: The sequential learning problem. In *Psychology of learning and motivation*, volume 24, pages 109–165. Elsevier, 1989.
- [19] Pablo Moreno-Muñoz, Antonio Artés-Rodríguez, and Mauricio A Álvarez. Continual multi-task Gaussian processes. *arXiv preprint arXiv:1911.00002*, 2019.
- [20] Kevin P Murphy. *Machine learning: a probabilistic perspective*. MIT press, 2012.
- [21] Cuong V. Nguyen, Yingzhen Li, Thang D. Bui, and Richard E. Turner. Variational continual learning. In *International Conference on Learning Representations*, 2018.
- [22] Adam Paszke, Sam Gross, Francisco Massa, Adam Lerer, James Bradbury, Gregory Chanan, Trevor Killeen, Zeming Lin, Natalia Gimelshein, Luca Antiga, Alban Desmaison, Andreas Kopf, Edward Yang, Zachary DeVito, Martin Raison, Alykhan Tejani, Sasank Chilamkurthy, Benoit Steiner, Lu Fang, Junjie Bai, and Soumith Chintala. Pytorch: An imperative style, high-performance deep learning library. In *Advances in Neural Information Processing Systems 32*, pages 8024–8035. 2019.
- [23] Joaquin Quiñonero-Candela and Carl Edward Rasmussen. A unifying view of sparse approximate Gaussian process regression. *Journal of Machine Learning Research*, 6(Dec):1939–1959, 2005.
- [24] Carl Edward Rasmussen and Christopher K. I. Williams. *Gaussian Processes for Machine Learning (Adaptive Computation and Machine Learning)*. The MIT Press, 2005.
- [25] Roger Ratcliff. Connectionist models of recognition memory: constraints imposed by learning and forgetting functions. *Psychological review*, 97(2):285, 1990.
- [26] Sylvestre-Alvise Rebuffi, Alexander Kolesnikov, Georg Sperl, and Christoph H Lampert. iCaRL: Incremental classifier and representation learning. In *Proceedings of the IEEE conference on Computer Vision and Pattern Recognition*, pages 2001–2010, 2017.
- [27] Mark Bishop Ring. *Continual learning in reinforcement environments*. PhD thesis, University of Texas at Austin, 1994.

- [28] Hippolyt Ritter, Aleksandar Botev, and David Barber. Online structured Laplace approximations for overcoming catastrophic forgetting. In *Advances in Neural Information Processing Systems*, pages 3738–3748, 2018.
- [29] Andrei A Rusu, Neil C Rabinowitz, Guillaume Desjardins, Hubert Soyer, James Kirkpatrick, Koray Kavukcuoglu, Razvan Pascanu, and Raia Hadsell. Progressive neural networks. *URL* <http://arxiv.org/abs/1606.04671>, 2016.
- [30] Masa-Aki Sato. Online model selection based on the variational Bayes. *Neural computation*, 13(7):1649–1681, 2001.
- [31] Jonathan Schwarz, Jelena Luketina, Wojciech M Czarnecki, Agnieszka Grabska-Barwinska, Yee Whye Teh, Razvan Pascanu, and Raia Hadsell. Progress & compress: A scalable framework for continual learning. *arXiv preprint arXiv:1805.06370*, 2018.
- [32] Jiaxin Shi, Michalis K. Titsias, and Andriy Mnih. Sparse orthogonal variational inference for Gaussian processes. In *Artificial Intelligence and Statistics*, 2020.
- [33] Hanul Shin, Jung Kwon Lee, Jaehong Kim, and Jiwon Kim. Continual learning with deep generative replay. In *Advances in Neural Information Processing Systems*, pages 2990–2999, 2017.
- [34] Siddharth Swaroop, Cuong V. Nguyen, Thang D. Bui, and Richard E. Turner. Improving and understanding variational continual learning. *arXiv:1905.02099 [cs, stat]*, 2019.
- [35] Sebastian Thrun. Lifelong learning algorithms. In *Learning to learn*, pages 181–209. Springer, 1998.
- [36] Michalis Titsias. Variational learning of inducing variables in sparse Gaussian processes. In *Artificial Intelligence and Statistics*, pages 567–574, 2009.
- [37] Michalis K Titsias, Jonathan Schwarz, Alexander G de G Matthews, Razvan Pascanu, and Yee Whye Teh. Functional regularisation for continual learning with Gaussian processes. In *International Conference on Learning Representations*, 2020.
- [38] Gido M van de Ven and Andreas S Tolias. Three scenarios for continual learning. *arXiv preprint arXiv:1904.07734*, 2019.
- [39] Florian Wenzel, Kevin Roth, Bastiaan S Veeling, Jakub Świątkowski, Linh Tran, Stephan Mandt, Jasper Snoek, Tim Salimans, Rodolphe Jenatton, and Sebastian Nowozin. How good is the Bayes posterior in deep neural networks really? *arXiv preprint arXiv:2002.02405*, 2020.
- [40] Andrew Gordon Wilson, Zhiting Hu, Ruslan Salakhutdinov, and Eric P Xing. Deep kernel learning. In *Artificial Intelligence and Statistics*, pages 370–378, 2016.
- [41] Manzil Zaheer, Sashank Reddi, Devendra Sachan, Satyen Kale, and Sanjiv Kumar. Adaptive methods for nonconvex optimization. In *Advances in Neural Information Processing Systems*, pages 9793–9803, 2018.
- [42] Friedemann Zenke, Ben Poole, and Surya Ganguli. Continual learning through synaptic intelligence. In *34th International Conference on Machine Learning*, pages 3987–3995, 2017.

A VAR-GP Pseudocode

Algorithm 1 summarizes the training loop for a task at time t .

Algorithm 1: VAR-GP per-task training

Input: Learning rate η , Batch size B , Number of inducing points M , Maximum epochs E , Task dataset $\mathcal{D}^{(t)}$, hyperparameters KL tempering factor β , Early stopping patience of K epochs and tolerance δ

Output: Per-task kernel hyper-parameters θ_t , inducing points \mathbf{Z}_t and function values \mathbf{u}_t
 // subset of training data as initial inducing points

```

1 Initialize  $\mathbf{Z}_t \in \mathbb{R}^{M \times D} \subset \mathcal{D}^{(t)} \in \mathbb{R}^{N_t \times D}$ 
2 for  $e$  in  $1 \dots E$  do
3   for  $\{\mathbf{x}_i, y_i\}_{i=1}^B \subset \mathcal{D}^{(t)}$  do
4     Compute  $\mathcal{F}(q_t)$  - either (6) or (9)
5     Update  $\theta_t$ ,  $\mathbf{u}_t$  and  $\mathbf{Z}_t$  with learning rate  $\eta$  and tempering factor  $\beta$ 
6   Compute validation accuracy  $A_e$ 
7   if  $e > K$  and  $|A_e - A_{e-K}| < \delta$  then
8     break // early stopping
```

A.1 Posterior Predictive

For a novel input \mathbf{x}_* , the posterior predictive is computed via a Monte Carlo approximation of

$$p(y_* | \mathbf{x}_*) = \int p(y_* | f) q_t(f, \theta | \mathbf{x}_*) df d\theta \quad (10)$$

For a K -way classifier, we train K independent GPs and use the Bayes optimal prediction $\operatorname{argmax}_i p(y_*^{(i)} | \mathbf{x}_*), i \in \{1, \dots, K\}$ to compute accuracies.

B Ablations

B.1 Global Inducing Points

This section outlines the assumptions made for the ablation titled as ‘‘Global’’. The characterization for the first task remains the same as in VAR-GPs. For subsequent tasks, the general model and the variational assumption is written as (with implicit dependence on \mathbf{Z}),

$$p(\mathbf{y}^{(t)}, f, \theta | \mathbf{X}^{(t)}, \mathcal{D}^{(<t)}) \approx q_{t-1}(\theta) q(\mathbf{u}_{t-1}) p(f_{\neq \mathbf{u}_{t-1}} | \mathbf{X}^{(t)}, \mathbf{u}_{t-1}, \theta) \prod_{i=1}^{N_t} p(y_i^{(t)} | f, \mathbf{x}_i^{(t)}), \quad (11)$$

$$q_t(f, \theta) = q_t(\theta) q(\mathbf{u}_t) p(f_{\neq \mathbf{u}_t} | \mathbf{X}^{(t)}, \mathbf{u}_t, \theta). \quad (12)$$

Note that we don’t have the auto-regressive characterization of VAR-GPs in the model anymore and instead have an approximate dependence through the variational posterior for the previous task. We further note that

$$p(f_{\neq \mathbf{u}_{t-1}} | \mathbf{X}^{(t)}, \mathbf{u}_{t-1}, \theta) = p(f_{\neq \mathbf{u}_{t-1}, \mathbf{u}_t} | \mathbf{X}^{(t)}, \mathbf{u}_{t-1}, \mathbf{u}_t, \theta) \frac{p(\mathbf{u}_{t-1}, \mathbf{u}_t | \theta)}{p(\mathbf{u}_{t-1} | \theta)}, \quad (13)$$

$$p(f_{\neq \mathbf{u}_t} | \mathbf{X}^{(t)}, \mathbf{u}_t, \theta) = p(f_{\neq \mathbf{u}_{t-1}, \mathbf{u}_t} | \mathbf{X}^{(t)}, \mathbf{u}_{t-1}, \mathbf{u}_t, \theta) \frac{p(\mathbf{u}_{t-1}, \mathbf{u}_t | \theta)}{p(\mathbf{u}_t | \theta)}. \quad (14)$$

Owing to key cancellations, the variational lower bound now is given by,

$$\begin{aligned}
\mathcal{F}(q_t) &= \sum_{i=1}^{N_t} \mathbb{E}_{q_t(f, \theta)} \left[\log p \left(y_i^{(t)} \mid f, \mathbf{x}_i^{(t)} \right) \right] \\
&\quad - \mathcal{KL} \left[q_t(\theta) \parallel q_{t-1}(\theta) \right] - \mathbb{E}_{q_t(\theta)} \left[\mathcal{KL} \left[q(\mathbf{u}_t) \parallel p(\mathbf{u}_t \mid \theta) \right] \right] \\
&\quad + \mathbb{E}_{q_t(\theta) q(\mathbf{u}_t \mid \theta) p(\mathbf{u}_{t-1} \mid \mathbf{u}_t, \theta)} \left[\log \frac{q(\mathbf{u}_{t-1})}{p(\mathbf{u}_{t-1} \mid \theta)} \right]. \tag{15}
\end{aligned}$$

A key difference to note here is that the \mathcal{KL} regularizer containing inducing points \mathbf{u}_t is not conditional on the previous ones anymore.

B.2 Re-VAR-GP: Retraining old inducing points

In this version of VAR-GP, we allow retraining of old inducing points and call it Retractable VAR-GP (abbreviated as Re-VAR-GP). We clarify the precise nature of terms. Leading from (7) and (9), we highlight frozen $\tilde{\mathbf{u}}_{<t}$ and $\tilde{\mathbf{Z}}_{<t}$ (with a tilde) in the prior model to differentiate against learnable parameters:

$$\begin{aligned}
p(\mathbf{y}^{(t)}, f, \theta \mid \mathbf{X}^{(t)}, \mathcal{D}^{(<t)}) &\approx q_{t-1}(\theta) q(\tilde{\mathbf{u}}_{<t} \mid \tilde{\mathbf{Z}}_{<t}, \theta) p(\mathbf{u}_t \mid \mathbf{Z}_t, \tilde{\mathbf{u}}_{<t}, \tilde{\mathbf{Z}}_{<t}, \theta) \\
&\quad p(f_{\neq \mathbf{u}_t, \tilde{\mathbf{u}}_{<t}} \mid \mathbf{X}^{(t)}, \mathbf{u}_t, \tilde{\mathbf{u}}_{<t}, \mathbf{Z}_t, \tilde{\mathbf{Z}}_{<t}, \theta) \prod_{i=1}^{N_t} p(y_i^{(t)} \mid f, \mathbf{x}_i^{(t)}). \tag{16}
\end{aligned}$$

We posit the variational posterior as

$$q_t(f, \theta) = q_t(\theta) q(\mathbf{u}_{<t} \mid \mathbf{Z}_{<t}, \theta) q(\mathbf{u}_t \mid \mathbf{Z}_t, \mathbf{u}_{<t}, \mathbf{Z}_{<t}, \theta) p(f_{\neq \mathbf{u}_t, \mathbf{u}_{<t}} \mid \mathbf{X}^{(t)}, \mathbf{u}_t, \mathbf{u}_{<t}, \mathbf{Z}_t, \mathbf{Z}_{<t}, \theta). \tag{17}$$

To simplify these equations, we note the following identities.

$$\begin{aligned}
p(f_{\neq \mathbf{u}_t, \mathbf{u}_{<t}} \mid \mathbf{X}^{(t)}, \mathbf{u}_t, \mathbf{u}_{<t}, \mathbf{Z}_t, \mathbf{Z}_{<t}, \theta) &= p(f_{\neq \mathbf{u}_t, \mathbf{u}_{<t}, \tilde{\mathbf{u}}_{<t}} \mid \mathbf{X}^{(t)}, \mathbf{u}_t, \mathbf{u}_{<t}, \tilde{\mathbf{u}}_{<t}, \mathbf{Z}_t, \mathbf{Z}_{<t}, \tilde{\mathbf{Z}}_{<t}, \theta) \\
&\quad p(\tilde{\mathbf{u}}_{<t} \mid \mathbf{u}_t, \mathbf{u}_{<t}, \mathbf{Z}_t, \mathbf{Z}_{<t}, \tilde{\mathbf{Z}}_{<t}, \theta), \tag{18}
\end{aligned}$$

$$\begin{aligned}
p(f_{\neq \mathbf{u}_t, \tilde{\mathbf{u}}_{<t}} \mid \mathbf{X}^{(t)}, \mathbf{u}_t, \tilde{\mathbf{u}}_{<t}, \mathbf{Z}_t, \tilde{\mathbf{Z}}_{<t}, \theta) &= p(f_{\neq \mathbf{u}_t, \mathbf{u}_{<t}, \tilde{\mathbf{u}}_{<t}} \mid \mathbf{X}^{(t)}, \mathbf{u}_t, \mathbf{u}_{<t}, \tilde{\mathbf{u}}_{<t}, \mathbf{Z}_t, \mathbf{Z}_{<t}, \tilde{\mathbf{Z}}_{<t}, \theta) \\
&\quad p(\mathbf{u}_{<t} \mid \mathbf{u}_t, \tilde{\mathbf{u}}_{<t}, \mathbf{Z}_t, \mathbf{Z}_{<t}, \tilde{\mathbf{Z}}_{<t}, \theta), \tag{19}
\end{aligned}$$

$$\frac{p(\mathbf{u}_t \mid \mathbf{Z}_t, \tilde{\mathbf{u}}_{<t}, \tilde{\mathbf{Z}}_{<t}, \theta) p(\mathbf{u}_{<t} \mid \mathbf{u}_t, \tilde{\mathbf{u}}_{<t}, \mathbf{Z}_t, \mathbf{Z}_{<t}, \tilde{\mathbf{Z}}_{<t}, \theta)}{p(\tilde{\mathbf{u}}_{<t} \mid \mathbf{u}_t, \mathbf{u}_{<t}, \mathbf{Z}_t, \mathbf{Z}_{<t}, \tilde{\mathbf{Z}}_{<t}, \theta)} = \frac{p(\mathbf{u}_{<t}, \mathbf{u}_t \mid \mathbf{Z}_t, \mathbf{Z}_{<t}, \theta)}{p(\tilde{\mathbf{u}}_{<t} \mid \tilde{\mathbf{Z}}_{<t}, \theta)}. \tag{20}$$

Using these identities, the lower bound now simplifies as

$$\begin{aligned}
\mathcal{F}(q_t) &= \sum_{i=1}^{N_t} \mathbb{E}_{q_t(f, \theta)} \left[\log p \left(y_i^{(t)} \mid f, \mathbf{x}_i^{(t)} \right) \right] \\
&\quad - \mathcal{KL} \left[q_t(\theta) \parallel q_{t-1}(\theta) \right] \\
&\quad - \mathbb{E}_{q_t(\theta)} \left[\mathcal{KL} \left[q(\mathbf{u}_{\leq t} \mid \mathbf{Z}_{\leq t}, \theta) \parallel p(\mathbf{u}_{\leq t} \mid \mathbf{Z}_{\leq t}, \theta) \right] \right] \\
&\quad - \mathbb{E}_{q_t(\theta) q(\mathbf{u}_{\leq t} \mid \mathbf{Z}_{\leq t}, \theta) p(\tilde{\mathbf{u}}_{<t} \mid \tilde{\mathbf{Z}}_{<t}, \mathbf{u}_{\leq t}, \mathbf{Z}_{\leq t}, \theta)} \left[\log \frac{p(\tilde{\mathbf{u}}_{<t} \mid \tilde{\mathbf{Z}}_{<t}, \theta)}{q(\tilde{\mathbf{u}}_{<t} \mid \tilde{\mathbf{Z}}_{<t}, \theta)} \right]. \tag{21}
\end{aligned}$$

The key differences to note here are the fact that prior model now conditions on the frozen inducing points while the new variational distributions introduced are still free to optimize those points further. This leads to additional terms in the variational lower bound. We briefly discuss the performance next.

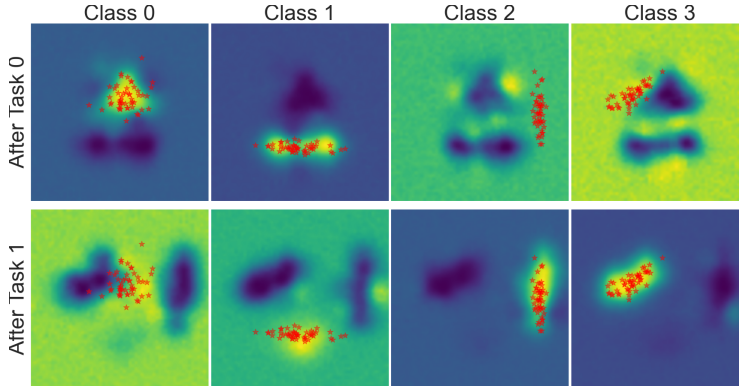


Figure 6: This figure shows class-wise output probabilities in each column for classifiers trained using a synthetic dataset (Fig. 2) on the 2-D plane $x, y \in [-3., 3.]$. The first row represents the density surface after training for Task 0 (observing classes 0/1) and the second after training for Task 1 (observing classes 2/3). Brighter regions represent higher probabilities. Training points for each class are marked (*). Re-VAR-GP tends to suffer from catastrophic forgetting. Notice the approximately uniform uncertainty in regions for Class 0 and Class 1 after training on the second task.

B.2.1 Performance on Toy Dataset

Similar in spirit to Fig. 1, we train Re-VAR-GP on the toy dataset in Fig. 2. The density plots for training after both first task (training on classes 0/1) and the second (training on classes 2/3) are presented in Fig. 6.

As shown in Fig. 6, Re-VAR-GP is not able to retain the information gained from previous task, a sign of catastrophic forgetting. This can be understood from the nature of the lower bound in (21). The only term that can potentially contribute to preservation of old information is the expected ratio $\log \frac{p(\tilde{\mathbf{u}}_{\leq t} | \tilde{\mathbf{Z}}_{\leq t}, \theta)}{q(\tilde{\mathbf{u}}_{\leq t} | \tilde{\mathbf{Z}}_{\leq t}, \theta)}$. However, this term avoids any interaction between $\tilde{\mathbf{u}}_{\leq t}$ and $\mathbf{u}_{\leq t}$. As a result, the retrainable parameters $\mathbf{u}_{\leq t}$ and $\mathbf{Z}_{\leq t}$ have no information-preserving regularization unlike VAR-GPs as seen in (9). Owing to this observation, we do not pursue this model further.

B.3 Deep Kernel Learning

For increased representational power in the kernel, we also provide preliminary experiments with Deep Kernel Learning [40]. Effectively, we augment the Exponentiated Quadratic kernel with a feature extractor $f_\phi(x)$ in the form of a neural network and allow them to be trained with additional kernel hyperparameters ϕ . This amounts to replacing \mathbf{x} and \mathbf{x}' in (22) with $f_\phi(\mathbf{x})$ and $f_\phi(\mathbf{x}')$ respectively. We only use point estimates for ϕ , initialized at the previous task $\forall t > 1$.

B.3.1 Experiments with Split MNIST

We use a neural network with two hidden layers of size 256 each and the final output feature size of 64 to parameterize f_ϕ and train the system end-to-end. As we see in Fig. 7, the performance declines much faster than in VAR-GPs.

This result hints towards weak regularization of the feature extractor as we encounter subsequent tasks. The introduction of a neural network makes the inference problem much harder and any potential remedies are beyond the scope of current work. We, therefore, do not discuss this further but makes for an exciting direction to pursue in the future.

C Implementation

C.1 Exponentiated Quadratic kernel

The precise parametrization of the kernel used is given below. $\|\cdot\|_2$ is the ℓ^2 -norm. We parameterize $\log \gamma$ and $\log \sigma$.

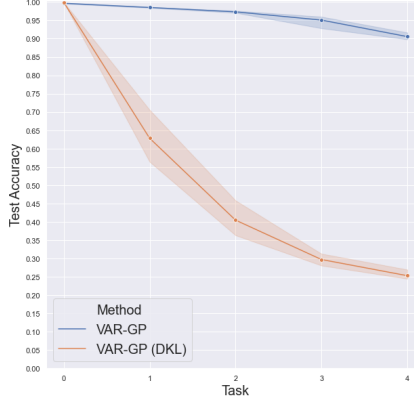


Figure 7: This figure shows the task-wise test accuracy on Split MNIST over five independent runs. We train a neural network as a feature extractor before applying the kernel (as described in §B.3). It is clear that the neural networks require stronger regularization as we incorporate more tasks.

$$k(\mathbf{x}, \mathbf{x}') = \gamma \exp \left\{ \frac{\|\mathbf{x} - \mathbf{x}'\|_2^2}{2\sigma^2} \right\} \quad (22)$$

C.2 Parameterizing covariance matrices

In all experiments, we parameterize a covariance matrix $\Sigma \in \mathbb{R}^{M \times M}$ using its Cholesky decomposition $\Sigma = \mathbf{L}\mathbf{L}^\top$ where $\mathbf{L} \in \mathbb{R}^{M \times M}$ is a lower triangular matrix with positive diagonals. The positivity of the diagonals is maintained via a `softplus` transform. As a result, we can apply unconstrained optimization on $\frac{M \times (M+1)}{2}$ free parameters corresponding to the lower triangular matrix \mathbf{L} .

C.3 Computing the auto-regressive distributions in VAR-GPs

When using the auto-regressive parametrization in VAR-GPs, the joint distribution over all inducing points up to and including the current time step can be decomposed as follows,

$$q(\mathbf{u}_{\leq t} | \theta) = q(\mathbf{u}_{< t} | \theta) q(\mathbf{u}_t | \mathbf{u}_{< t}, \theta) = \mathcal{N}(\mathbf{u}_{< t}; \mathbf{m}_{< t}, \Sigma_{< t}) \mathcal{N}(\mathbf{u}_t; \mathbf{A}_t \mathbf{u}_{< t} + \mathbf{m}_t, \Sigma_t).$$

While we cannot avoid sampling the hyperparameters θ , we can avoid variance introduced by the ancestral sampling of variational distribution for computation of (9). We recognize that the full auto-regressive distribution can be computed in closed form as it is a product Gaussians with linear dependence in the mean, similar in spirit to linear Gaussian dynamical systems [20].

$$\begin{aligned} q(\mathbf{u}_{\leq t} | \theta) &= q(\mathbf{u}_{< t}) q(\mathbf{u}_t | \theta) && (\forall t > 1) \\ &= \mathcal{N}(\mathbf{u}_{< t}; \mathbf{m}_{< t}, \Sigma_{< t}) \mathcal{N}(\mathbf{u}_t; \mathbf{A}_t \mathbf{u}_{< t} + \mathbf{m}_t, \Sigma_t) && (\mathbf{A}_t = \mathbf{K}_{\mathbf{z}_t, \mathbf{z}_{< t}} \mathbf{K}_{\mathbf{z}_{< t}, \mathbf{z}_{< t}}^{-1}) \\ &= \mathcal{N} \left(\begin{bmatrix} \mathbf{u}_{< t} \\ \mathbf{u}_t \end{bmatrix}; \begin{bmatrix} \mathbf{m}_{< t} \\ \mathbf{A}_t \mathbf{m}_{< t} + \mathbf{m}_t \end{bmatrix}, \begin{bmatrix} \Sigma_{< t} & \Sigma_{< t} \mathbf{A}_t^\top \\ \mathbf{A}_t \Sigma_{< t}^\top & \Sigma_t + \mathbf{A}_t \Sigma_{< t} \mathbf{A}_t^\top \end{bmatrix} \right) \end{aligned} \quad (23)$$

D Hyperparameters

D.1 Search Space

The search space for all hyperparameters used across experiments is described in Table 2. Top hyperparameters were picked using a held-out validation set.

Table 2: List of key hyperparameters with relevant search spaces.

Hyperparameter	Range / Value
Learning Rate (η)	[0.001, 0.01]
Inducing Points (M)	[40, 200]
Hypers \mathcal{KL} Tempering Factor (β)	[1.0, 10.0]
Batch Size (B)	512
Maximum Epochs (E)	500
Early Stopping Patience Epochs (K)	200
Early Stopping Tolerance (δ)	0.0001